Journal of Solid State Chemistry 188 (2012) 66–71

Contents lists available at SciVerse ScienceDirect

Journal of Solid State Chemistry

journal homepage: www.elsevier.com/locate/jssc

Superconductivity in quaternary niobium oxynitrides containing main group elements (M=Mg, Al, Si)

Y. Ohashi [a], S. Kikkawa [a,*], I. Felner [b], M.I. Tsindlekht [b], D. Venkateshwarlu [c], V. Ganesan [c], J.V. Yakhmi [d]

[a] Faculty of Engineering, Hokkaido University, N13W8, Kita-ku, Sapporo 060-8628, Japan
[b] Racah Institute of Physics, The Hebrew University, Jerusalem 91904, Israel
[c] UGC-DAE-Consortium for Scientific Research, Khandwa Rd, Indore (MP) 452001, India
[d] Bhabha Atomic Research Centre, Mumbai 400085, India

ARTICLE INFO

Article history:
Received 4 December 2011
Received in revised form
8 January 2012
Accepted 10 January 2012
Available online 24 January 2012

Keywords:
Superconductor
Niobium oxynitride
Magnetic measurement
Heat capacity

ABSTRACT

Niobium compounds continue to be an interesting family of superconductors, with the recent addition of oxynitrides to it, which can be categorized as low-T_c superconductors (LTS) because they exhibit superconductivity below $T_c \sim 17$ K. In this paper, we report the superconducting properties of three members of the family of niobium oxynitrides, viz. $(Nb_{0.89}Al_{0.11})(N_{0.84}O_{0.16})$, $(Nb_{0.95}Mg_{0.05})(N_{0.92}O_{0.08})$ and $(Nb_{0.87}Si_{0.09}\square_{0.04})(N_{0.87}O_{0.13})$. Low temperature dc and ac magnetization measurements have been performed. In addition, heat capacity has been recorded at low temperature under applied magnetic fields. A detailed analysis of the data is presented.

1. Introduction

Superconductivity has been reported for several categories of niobium nitrides [1–7]: α-NbN_x ($0 \le x \le 0.40$) is a superconductor with the transition temperature, T_c=4.0–9.2 K; β-Nb_2N, crystallizing in hexagonal ε-Fe_2N type structure has T_c=3.8–8.6 K; and higher nitrides, which crystallize in rock-salt type structure, have fairly high T_c values, viz. γ-Nb_4N_3 (T_c=12–15 K), δ-NbN (T_c=14.7–17.7 K) and Nb_4N_5 (T_c=8.5–10 K). On the other hand, δ′-NbN and ε-NbN which crystallize in NiAs and TiP type structures, respectively, are non-superconductors.

In view of the high value of T_c obtained for δ-NbN, attempts have been made to prepare its solid solution derivatives by partial substitution of transition metals at Nb-site, using different synthesis routes such as ammonolysis, high temperature reaction under nitrogen, or solid state reaction of transition metal nitrides [8,9]. Measurements on them have shown that these derivatives are superconducting too, with T_c values intermediate between those for their end members, apparently due to the hybridization of their *d*-orbitals. Slight enhancement in T_c has been reported for the solid solution formed between δ-NbN and TiC, with $T_c \sim 18.0$ K [9]. However, there has been no report on doping of the main group elements in δ-NbN, especially their co-doping with oxide ions. With a view to obtain new oxynitrides of niobium, doping of both Al^{3+} and O^{2-} ions was attempted into the rock-salt structure of δ-NbN, which yielded the superconducting compound $(Nb_{0.89}Al_{0.11})(N_{0.84}O_{0.16})$ with T_c=17.3 K [10]. This compound, with a simple rock-salt structure, was obtained after annealing in nitrogen at 1500 °C. The doped Al^{3+} ions, in this case, were assumed to form Al^{3+}–O^{2-} pairs in the rock-salt structure because of the similar contents in Al^{3+} and O^{2-} ions. These Al^{3+}–O^{2-} pairs are distributed statistically in the rock-salt type lattice in about $(1/2)^3$ concentration. Prior to this, a vacancy-ordered niobium aluminum oxynitride with a composition as refined to be $(Nb_{0.60}Al_{0.08}\square_{0.32})(N_{0.79}O_{0.21})$, was also prepared *via* ammonolysis of an oxide precursor, obtained through citrate route [11]. Most recently, we have synthesized Mg- and Si-doped niobium oxynitrides, too, by post-annealing of the ammonolysis products in nitrogen [12]. These oxynitrides also crystallized with a rock-salt type crystal structure, similar to δ-NbN, and exhibited superconductivity at $T_c > 16$ K. In particular, about 10% of the nitride ions were substituted with oxide ions, simultaneously with substitution of niobium by only Mg^{2+}, or Si^{4+}, leading obviously to some cationic vacancies.

The formulas, cell parameter values, and the T_c values of the four niobium oxynitrides being reported in the present study are as follows: (i) $Nb_{1.00}(N_{0.98}O_{0.02})$, a=0.442 nm, T_c=17.6 K; (ii) $(Nb_{0.95}Mg_{0.05})(N_{0.92}O_{0.08})$, a=0.4419 nm, T_c=17.0 K; (iii) $(Nb_{0.89}Al_{0.11})(N_{0.84}O_{0.16})$, a=0.4401 nm, T_c=16.7 K; and (iv) $(Nb_{0.87}Si_{0.09}\square_{0.04})(N_{0.87}O_{0.13})$, a=0.4399 nm, T_c=16.8 K. They

* Corresponding author. Fax: +81 11 706 6739.
E-mail address: kikkawa@eng.hokudai.ac.jp (S. Kikkawa).

0022-4596/$ - see front matter © 2012 Elsevier Inc. All rights reserved.
doi:10.1016/j.jssc.2012.01.024

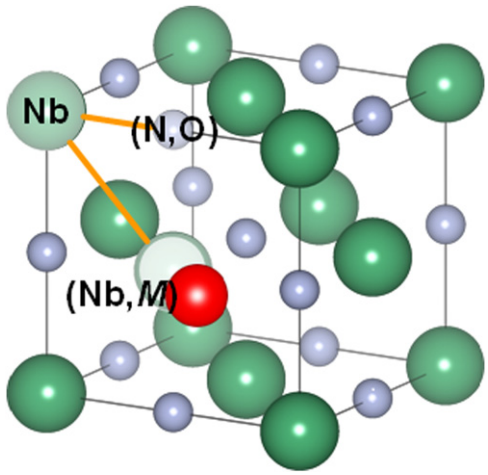

Fig. 1. The schematic of local structure around main group elements *M* in red sphere, especially Si-accompanied obvious cationic vacancies. The site for *M* shifts slightly from the regular octahedral to its neighboring tetrahedral one. (For interpretation of the references to color in this figure legend, the reader is referred to the web version of this article.)

were annealed in 0.5 MPa nitrogen atmosphere for 3 h at 1500 °C, except for the Si-doped sample which was annealed at 1200 °C, because it decomposed to a mixture of δ-NbN and SiO_2 at 1500 °C. Substitution of smaller-size Si^{4+}-ions at Nb-site introduces a large displacement at the octahedral 4*a* site, mainly because of the accompanied vacancy. Si^{4+}-ions may also get slightly shifted from the regular octahedral 4*a* site (shown in green in Fig. 1) towards the interstitial tetrahedral site (shown in red), statistically, in the rock-salt type lattice.

In the present study, superconducting properties were investigated on $(Nb_{0.89}Al_{0.11})(N_{0.84}O_{0.16})$, $(Nb_{0.95}Mg_{0.05})(N_{0.92}O_{0.08})$ and $(Nb_{0.87}Si_{0.09}\square_{0.04})(N_{0.87}O_{0.13})$. Effects of main group elements were studied on the superconducting properties through the measurements of low temperature dc and ac magnetization and heat capacity at low temperature under applied magnetic fields.

2. Experimental details

Synthesis methodology has already been described in Section 1. Temperature and field dependences of dc magnetization curves, $M(T)$ and $M(H_0)$, respectively, were recorded at various applied fields on powder samples, using a commercial MPMS5 Quantum Design SQUID magnetometer. A home-made ac-measurement setup has been adapted to this SQUID magnetometer, using which, the ac susceptibility was measured in arbitrary units with the pick-up coil method at amplitude $h_0=0.05$ Oe and frequencies of 819 and 1092 Hz. Heat capacity measurements were carried out on $(Nb_{0.89}Al_{0.11})(N_{0.84}O_{0.16})$, $(Nb_{0.95}Mg_{0.05})(N_{0.92}O_{0.08})$ and $(Nb_{0.87}Si_{0.09}\square_{0.04})(N_{0.87}O_{0.13})$ using Quantum Design PPMS system with relaxation method, down to 2 K and in the presence of magnetic fields up to 14 T. Mass of the samples used for these heat capacity measurements were 21, 19.2 and 15.7 mg, respectively.

3. Results and discussion

3.1. Magnetic measurements on $Nb_{1.00}(N_{0.98}O_{0.02})$, $(Nb_{0.95}Mg_{0.05})(N_{0.92}O_{0.08})$, $(Nb_{0.89}Al_{0.11})(N_{0.84}O_{0.16})$, and $(Nb_{0.87}Si_{0.09}\square_{0.04})(N_{0.87}O_{0.13})$

Fig. 2(a)–(d) shows the temperature dependence of the real (χ') and imaginary (χ'') ac susceptibility for all four samples, viz. $Nb_{1.00}(N_{0.98}O_{0.02})$, $(Nb_{0.95}Mg_{0.05})(N_{0.92}O_{0.08})$, $(Nb_{0.89}Al_{0.11})(N_{0.84}O_{0.16})$, and $(Nb_{0.87}Si_{0.09}\square_{0.04})(N_{0.87}O_{0.13})$. It is readily observed that the doped samples have lower T_c values, which was also observed by us before [12]. We also recorded the zero-field-cooled (ZFC) and field-cooled (FC) dc magnetization $M(T)$ curves at 8.8 Oe for the annealed Si-doped (data not shown). We used this dc $M(T)$ data to estimate the shielding volume fraction, from the ZFC branch as ~95%, which agrees well with ~95% value reported in our previous publication [12], where the estimated volume fractions for Al and Mg doped samples were reported to be 91% and 100%.

Fig. 3 presents the isothermal hysteresis loops $M(H)$, measured at 5 K for all four samples. From the hysteresis loop width (ΔM) at a given H, a rough estimate of the critical current density (J_C) can be made by using Bean's critical state model [13] for powders: $J_C=40\Delta M/3a$, where a is the average grain dimension. The interesting fact emerging from Fig. 3 is that J_C for $(Nb_{0.87}Si_{0.09}\square_{0.04})(N_{0.87}O_{0.13})$ is about 4 times larger than that of the rest of the samples. The estimated J_C at 5 K for this sample, for $H=1$ T and $a=0.01$ cm, is $\sim 2.5\times10^4$ A/cm^2. It is likely that the cation vacancies induced by doping silicon act as additional pinning centers. However, this value is two orders of magnitude lower (at least) than that of Nb_3Sn [14], indicating that the current sample is not much useful for applications even at temperatures as low as 5 K. The linear dependence of ΔM, and therefore, of J_C for $(Nb_{0.87}Si_{0.09}\square_{0.04})(N_{0.87}O_{0.13})$, at three different H values, is exhibited in Fig. 4. Similar trends were obtained for the other three materials.

X-ray absorption spectroscopy studies have shown [12] that the niobium *K*-edge shape was quite similar for the doped and undoped niobium oxynitrides. The first and the second nearest neighbors around Nb were observed at around 0.17 nm and 0.27 nm, respectively, for all samples measured [12], as compared to the literature values of 0.22 nm for Nb–(O,N) and 0.35 nm for Nb–Nb assuming a phase shift [7,11]. The peak profile was slightly broader in the case of the first and the second nearest neighbors for $(Nb_{0.87}Si_{0.09}\square_{0.04})(N_{0.87}O_{0.13})$ than those for the other three oxynitrides, possibly because the doping of silicon causes a relatively large displacement at the octahedral 4*a* site in the crystal structure. Our x-ray absorption study has not yet a clear picture of the coordination around Si. We are pursuing to elucidate this aspect by planning to record XAFS spectra for Mg, Al and Si for our Nb oxynitrides to throw light on the local atomic order. These elements are light and their net content per formula unit is not much, nor they form any particular crystal structure, all of which makes the analysis of spectra quite tough.

3.2. Heat capacity measurements on $(Nb_{0.89}Al_{0.11})(N_{0.84}O_{0.16})$, $(Nb_{0.95}Mg_{0.05})(N_{0.92}O_{0.08})$ and $(Nb_{0.87}Si_{0.09}\square_{0.04})(N_{0.87}O_{0.13})$

Measurement of heat capacity of a superconducting sample is expected to yield information regarding transition temperatures, critical fields, energy gap as well as on electron correlations. In our study, calorimetric measurements were conducted on the three oxynitrides $(Nb_{0.89}Al_{0.11})(N_{0.84}O_{0.16})$, $(Nb_{0.95}Mg_{0.05})(N_{0.92}O_{0.08})$ and $(Nb_{0.87}Si_{0.09}\square_{0.04})(N_{0.87}O_{0.13})$. The transitions (jumps) in the heat capacity curves in zero fields, can be taken as T_c values for the three samples. Fig. 5 shows a systematic trend in the plots of heat capacity divided by temperature (C/T) vs. T^2 under different values of applied magnetic fields. There is uniform decrease of T_c values upon application of magnetic fields in each case, and the jump at T_c gradually decreases, as expected.

Just above T_c, the heat capacity values are quite linear, as expected. Main contributions to the heat capacity can be obtained by fitting the normal state with the equation, $C=\gamma T+\beta T^3$, where γT and βT^3 have their usual meaning of electronic and phononic contributions, respectively. Extrapolating the normal state heat

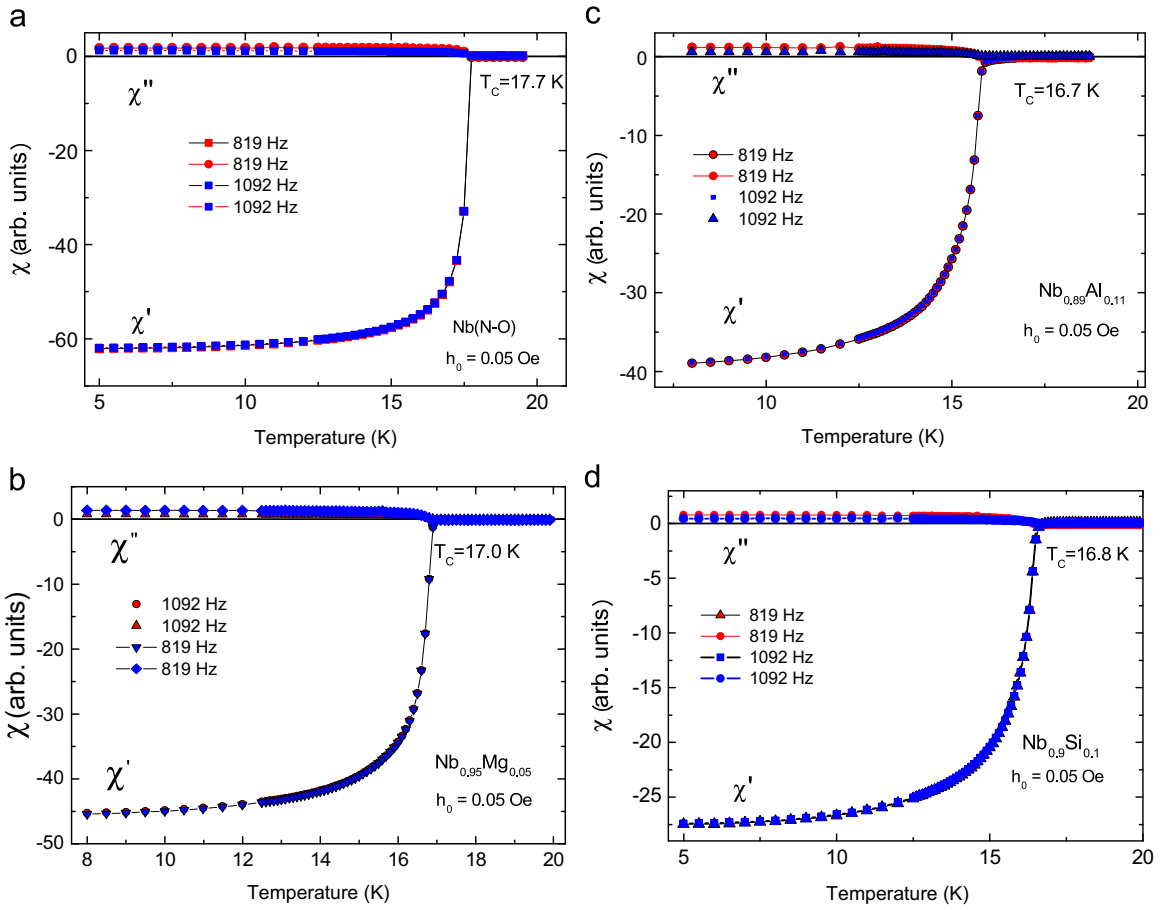

Fig. 2. The ac susceptibility data χ' vs. T and χ'' vs. T for (a) $Nb_{1.00}(N_{0.98}O_{0.02})$; (b) $(Nb_{0.95}Mg_{0.05})(N_{0.92}O_{0.08})$; (c) $(Nb_{0.89}Al_{0.11})(N_{0.84}O_{0.16})$, and (d) $(Nb_{0.87}Si_{0.09}\square_{0.04})(N_{0.87}O_{0.13})$ taken at two different frequencies 819 Hz and 1092 Hz.

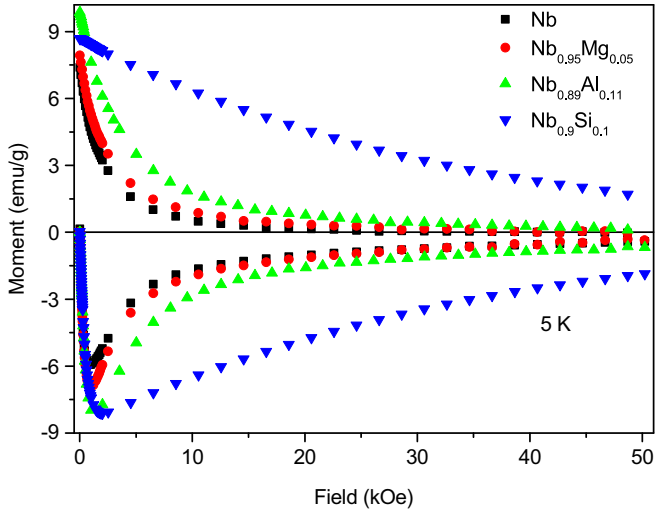

Fig. 3. Isothermal hysteresis loops at 5 K of the dc magnetization up to 5 T, for all the four samples: $Nb_{1.00}(N_{0.98}O_{0.02})$; $(Nb_{0.95}Mg_{0.05})(N_{0.92}O_{0.08})$; $(Nb_{0.89}Al_{0.11})(N_{0.84}O_{0.16})$, and $(Nb_{0.87}Si_{0.09}\square_{0.04})(N_{0.87}O_{0.13})$, nicknamed Nb, $Nb_{0.95}Mg_{0.05}$, $Nb_{0.89}Al_{0.11}$ and $Nb_{0.9}Si_{0.1}$, respectively.

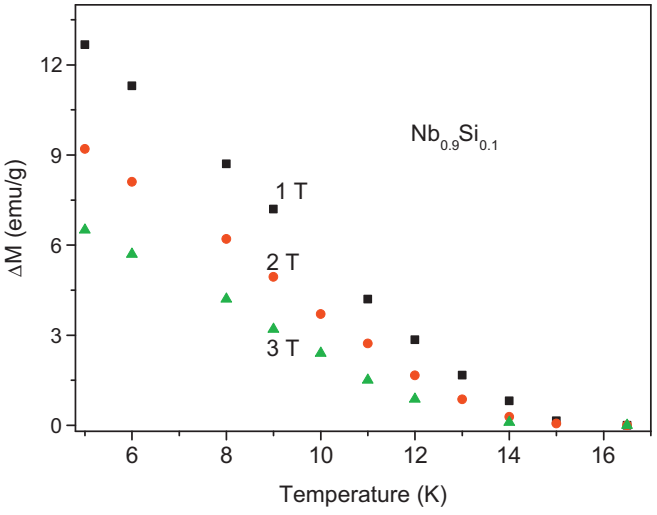

Fig. 4. Temperature dependence of ΔM for $(Nb_{0.87}Si_{0.09}\square_{0.04})(N_{0.87}O_{0.13})$, measured at 1, 2 and 3 T.

capacity to zero and fitting yields a γ value, which is 2.944 mJ/mol-K^2, 0.18 mJ/mol-K^2 and 25.269 mJ/mol-K^2, respectively, for the samples $(Nb_{0.89}Al_{0.11})(N_{0.84}O_{0.16})$, $(Nb_{0.95}Mg_{0.05})(N_{0.92}O_{0.08})$ and $(Nb_{0.87}Si_{0.09}\square_{0.04})(N_{0.87}O_{0.13})$. The γ value is an indicator of the nature of correlations present in the system. We have repeated the measurements several times, and got reproducible data which makes us conclude that the lattice contribution does not change much upon doping, and it is the electron correlations which are important for these samples. A value of $\gamma \sim 3$ mJ/mol-K^2 for $(Nb_{0.89}Al_{0.11})(N_{0.84}O_{0.16})$ is slightly higher than the free electron value of copper. This implies the onset of weak correlations and may be attributed to the carriers introduced by the Al-dopant. On the other hand, the Nb–Si sample shows a high value of $\gamma \sim 25$ mJ/mol-K^2, indicating strong correlations, which is a

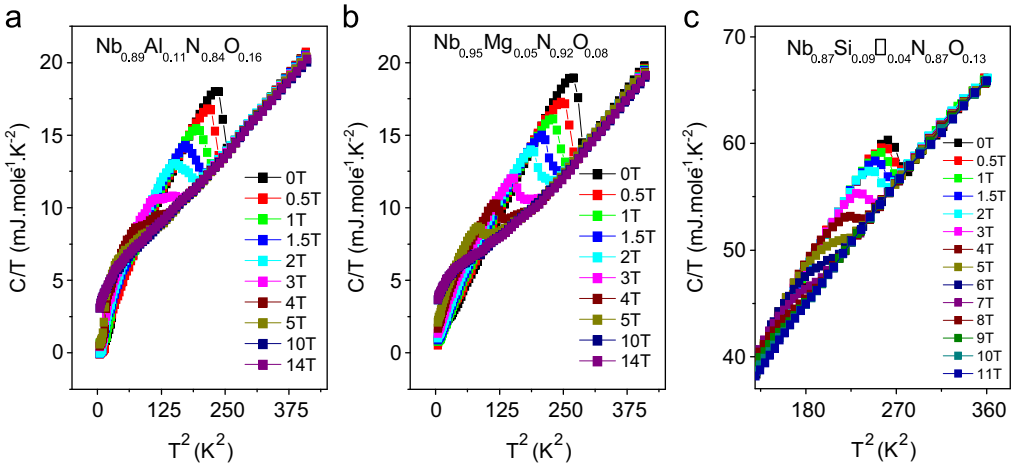

Fig. 5. Plots of C/T vs. T^2: (a) $(Nb_{0.89}Al_{0.11})(N_{0.84}O_{0.16})$; (b) $(Nb_{0.95}Mg_{0.05})(N_{0.92}O_{0.08})$ and (c) $(Nb_{0.87}Si_{0.09}\square_{0.04})(N_{0.87}O_{0.13})$. γT and βT^3 were estimated from the linear regions of the plots.

revealing observation. This also corroborates our ideas that there are fewer cation vacancies present in $(Nb_{0.89}Al_{0.11})(N_{0.84}O_{0.16})$; than in $(Nb_{0.87}Si_{0.09}\square_{0.04})(N_{0.87}O_{0.13})$ because the positive charge introduced by the Al^{3+} substitution cannot be fully neutralized by the co-doped O^{2-}. Finally, a value of 0.1798 mJ/mol-K^2 for $(Nb_{0.95}Mg_{0.05})(N_{0.92}O_{0.08})$ is comparable to the free-electron value of γ, suggesting that the electrons that take part in this case are quite 'normal' in nature. A lot more needs to be understood why the T_c is as high as ~17 K and the C/T is still quite linear even up to 20 K, which we plan to investigate through further measurements.

In order to evaluate the energy gap values for these oxynitride samples and to investigate the magnitude of the heat capacity jump seen at their respective T_c values, we have performed a rigorous analysis of the heat capacity data recorded under applied fields (0 T, 2 T and 4 T), in the region of T_c [15], and our analysis is depicted in Fig. 6. Even though we have shown only representative plots of data taken under 0, 2 and 4 T applied fields, similar analyses were done for a number of intermediate values of applied magnetic fields, as well, and gave consistent results. The data below T_c were fitted using the BCS equation $C_e=(A/T)\exp(-\Delta/k_BT)$, while above T_c it is simply equal to γ. Entropy conservation is in principle followed in fixing the T_c, such that nearly equal points were kept on either side of T_c (black line). The equivalent $2\Delta/k_BT_c$ values for $(Nb_{0.89}Al_{0.11})(N_{0.84}O_{0.16})$ varies from 3.97 to 2.37. The corresponding numbers for $(Nb_{0.95}Mg_{0.05})(N_{0.92}O_{0.08})$ varies from 4.63 to 2.22 while for $(Nb_{0.87}Si_{0.09}\square_{0.04})(N_{0.87}O_{0.13})$, it varies as 3.05 – 2.85. The zero field values of $2\Delta/k_BT_c$ put these materials near the border-line of conventional (low-T_c) superconductors. However, their variation as a function of the applied field needs to be examined further, and is shown pictorially in Fig. 7a.

The heat capacity jump seen at T_c, i.e. $\Delta C/\gamma T_c$ varies 1.94–0.89 for $(Nb_{0.89}Al_{0.11})(N_{0.84}O_{0.16})$, 44.4–3.65 for $(Nb_{0.95}Mg_{0.05})(N_{0.92}O_{0.08})$ and 0.19–0.07 for $(Nb_{0.87}Si_{0.09}\square_{0.04})(N_{0.87}O_{0.13})$. It is evident that for $(Nb_{0.89}Al_{0.11})(N_{0.84}O_{0.16})$, the value of the jump is slightly higher than the expected BCS value of 1.43, but for $(Nb_{0.95}Mg_{0.05})(N_{0.92}O_{0.08})$ it exhibits an exorbitantly high value. This signifies that the Mg-doped sample is indeed a low carrier density system and hence its γ is very low. It may be noted that the parent oxynitride samples have a tendency to exhibit metal-to-insulator (MIT) transitions, and hence assuming a low carrier density appears logical. If this is so, and if the value of gamma for $(Nb_{0.95}Mg_{0.05})(N_{0.92}O_{0.08})$ is low, then the ratio $\Delta C/\gamma T_c$ will shoot up, which is indeed what has been observed. For the case of $(Nb_{0.87}Si_{0.09}\square_{0.04})(N_{0.87}O_{0.13})$, the $\Delta C/\gamma T_c$ value around 0.19 is astonishingly low, in spite of the fact that the $2\Delta/k_BT_c$ value for $(Nb_{0.87}Si_{0.09}\square_{0.04})(N_{0.87}O_{0.13})$, is around 3.1 (with not much change with change in fields), which is just below the BCS limit of 3.53.

For a further insight into the superconducting behavior of these oxynitrides, we have estimated the critical fields from the visible jumps seen at different values of the applied magnetic field. Although we have used both the 'onset' as well as the 'mid-point' of the transitions for this, the plots shown are with 'mid-point' as yard-stick only. Fig. 7c shows the variation of zero temperature critical fields for $(Nb_{0.89}Al_{0.11})(N_{0.84}O_{0.16})$, $(Nb_{0.95}Mg_{0.05})(N_{0.92}O_{0.08})$ and $(Nb_{0.87}Si_{0.09}\square_{0.04})(N_{0.87}O_{0.13})$ samples. The nature of variation appears to be linear near T_c, as expected. However, fittings equally well follow the BCS equation $H_c(T)=H_{c0}[1-(T/T_c)^2]$, which is used to estimate the values of the zero temperature critical field H_{c0}, which are 7.33 T, 8.32 T and 19.57 T for $(Nb_{0.89}Al_{0.11})(N_{0.84}O_{0.16})$, $(Nb_{0.95}Mg_{0.05})(N_{0.92}O_{0.08})$ and $(Nb_{0.87}Si_{0.09}\square_{0.04})(N_{0.87}O_{0.13})$ oxynitrides.

4. Conclusions

Our studies on the three Nb-oxynitrides, $(Nb_{0.89}Al_{0.11})(N_{0.84}O_{0.16})$, $(Nb_{0.95}Mg_{0.05})(N_{0.92}O_{0.08})$ and $(Nb_{0.87}Si_{0.09}\square_{0.04})(N_{0.87}O_{0.13})$, show them to be superconducting below ~17 K, with shielding volume fractions ranging between 90% and 100%. Critical current density (J_C) for the Si-doped sample is $\sim 2.5\times10^4$ A/cm^2 at 5 K, which though not a very impressive value for applications, is four times higher than the corresponding values for the Al- or Mg-doped samples. It is likely that the cation vacancies induced by doping silicon act as additional pinning centers. Heat capacity measurements on these three samples have thrown up some interesting features, viz. the parameter γ, the coefficient of the electronic contribution to the heat capacity, and an indicator of the nature of electron correlations in a system, has a high value of ~25 mJ/mol-K^2 in the case of the Si-doped sample, pointing to strong correlations in it, whereas a value of 3 mJ/mol-K^2 for the Al-doped sample, and 0.1798 mJ/mol-K^2 for the Mg-doped sample show that the latter two samples are behaving as nearly 'free electron' like systems. The zero field values of the energy-gap related parameter, $2\Delta/k_BT_c$, indicate that all the three samples belong to the border-line of conventional (low-T_c) superconductors, though the variation of this parameter under applied field needs to be examined further.

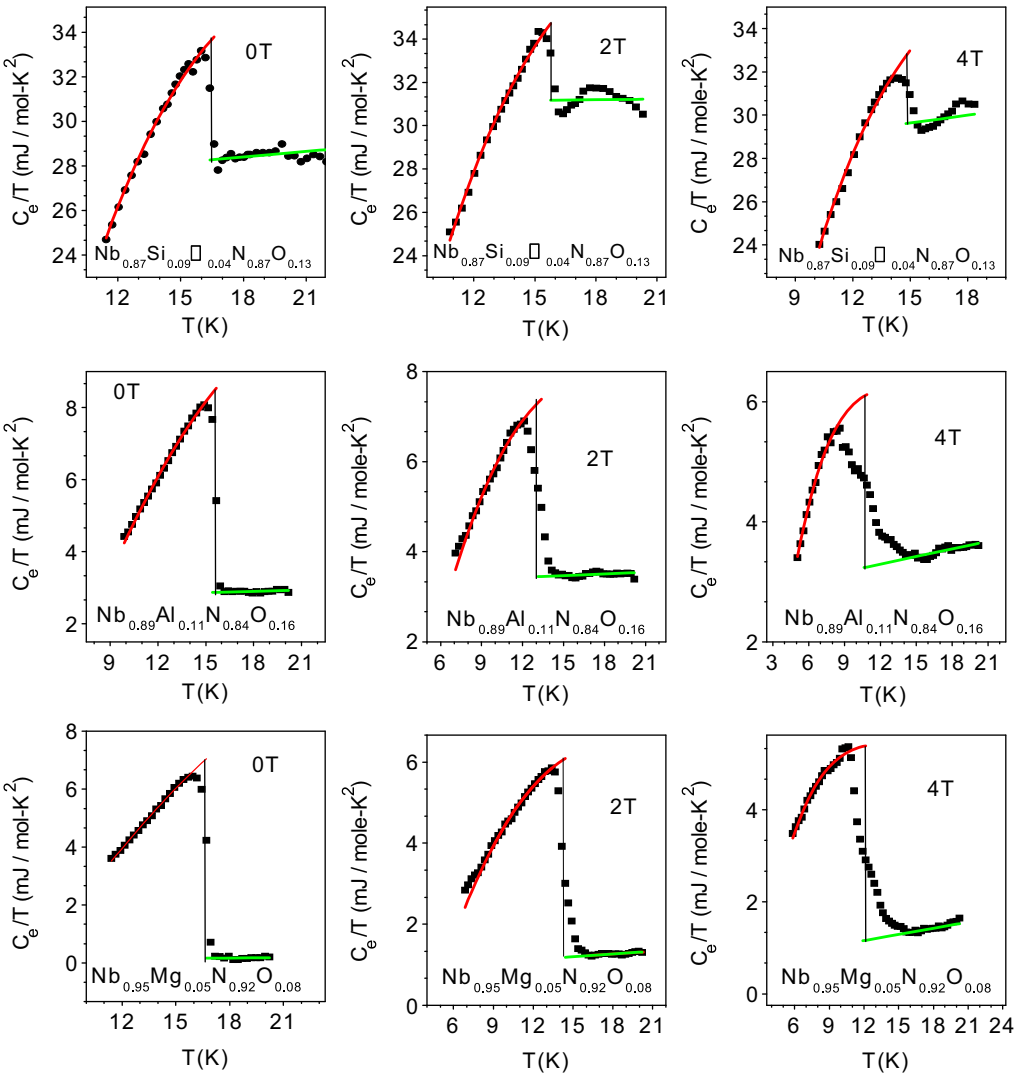

Fig. 6. Representative plots of C_e/T vs. T analysis for $(Nb_{0.87}Si_{0.09}\square_{0.04})(N_{0.87}O_{0.13})$, $(Nb_{0.89}Al_{0.11})(N_{0.84}O_{0.16})$ and $(Nb_{0.95}Mg_{0.05})(N_{0.92}O_{0.08})$. The data is obtained at three values of applied fields (0 T, 2 T and 4 T). Red lines below T_c are BCS fits to estimate the energy gap and the green lines above T_c are only a guide to the eye about the parameter γ. Vertical black lines denotes T_c. (For interpretation of the references to color in this figure legend, the reader is referred to the web version of this article.)

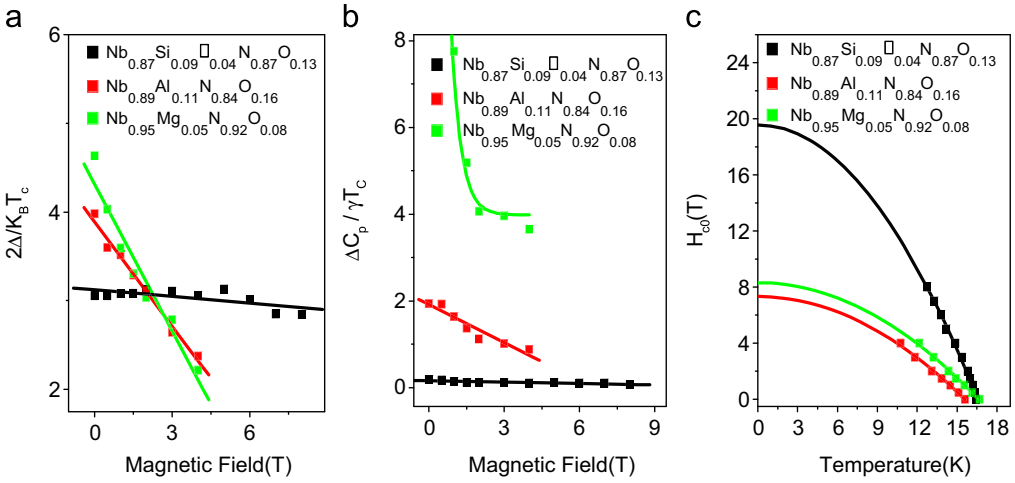

Fig. 7. Plots of (a) $2\Delta/k_BT_c$; (b) $\Delta C_p/\gamma T_c$, both as a function of magnetic fields; and (c) H_{c0} as a function of temperature, estimated from C_e/T vs. T analysis for $(Nb_{0.87}Si_{0.09}\square_{0.04})(N_{0.87}O_{0.13})$, $(Nb_{0.89}Al_{0.11})(N_{0.84}O_{0.16})$ and $(Nb_{0.95}Mg_{0.05})(N_{0.92}O_{0.08})$. The lines are only a guide to the eye for the plots (a) and (b). However, the lines in (c) represents BCS fits to the critical fields $H_c(T)=H_{c0}[1-(T/T_c)^2]$.

Acknowledgments

The research in Jerusalem is supported by the Klachky Foundation for Superconductivity. The research in Japan is supported by a Grant-in-Aid for Scientific Research (Kakenhi (A) #21245047) from the Japan Society for the Promotion of Science (JSPS).

References

[1] R.W. Guard, J.W. Savage, D.G. Swartout, Trans. Metall. Soc. AIME 239 (1967) 643–649.
[2] E.F. Skelton, M.R. Skokan, E. Cukauskas, J. Appl. Crystallogr. 14 (1981) 51–57.
[3] P. Fabbricatore, P. Fernandes, G.C. Gualco, F. Merlo, R. Musenich, R. Parodi, J. Appl. Phys. 66 (1989) 5944–5949.
[4] B. Scheerer, J. Cryst. Growth 49 (1980) 61–66.
[5] R. Berger, W. Lengauer, P. Ettmayer, J. Alloys Compd. 259 (1997) 9–13.
[6] A.V. Linde, R.-M. Marin-Ayral, D. Granier, F. Bosc-Rounessac, V.V. Grachev, Mater. Res. Bull. 44 (2009) 1025–1030.
[7] N. Terao, J. Less-Common Met. 23 (1971) 159–169.
[8] K. Hechler, G. Horn., G. Otto, E. Saur, J. Low Temp. Phys. 1 (1969) 29–43.
[9] N. Pessall, R.E. Gold, H.A. Johansen, J. Phys. Chem. Solids 29 (1968) 19–38.
[10] Y. Ohashi, T. Motohashi, Y. Masubuchi, S. Kikkawa, J. Solid State Chem. 183 (2010) 1710–1714.
[11] S. Yamamoto, Y. Ohashi, Y. Masubuchi, T. Takeda, T. Motohashi, S. Kikkawa, J. Alloys Compd. 482 (2009) 160–163.
[12] Y. Ohashi, T. Motohashi, Y. Masubuchi, T. Moriga, K. Murai, S. Kikkawa, J. Solid State Chem. 184 (2011) 2061–2065.
[13] E.M. Gyorgy, R.B. van Dover, K.A. Jackson, L.F. Schneemeyer, J.V. Waszczak, Appl. Phys. Lett. 55 (1989) 283.
[14] C.C. Tsuei, M. Suenaga, W.B. Sampson, Appl. Phys. Lett. 25 (1974) 318.
[15] G. Eguchi, D.C. Peets, M. Kriener, Y. Maeno, E. Nishibori, Y. Kumazawa, K. Banno, S. Maki, H. Sawa, Phys. Rev. B 83 (2011) 024512.